



All–solid–state quantum dot–sensitized solar cell from plastic crystal electrolyte

Journal:	<i>RSC Advances</i>
Manuscript ID:	RA-COM-03-2015-005275
Article Type:	Communication
Date Submitted by the Author:	25-Mar-2015
Complete List of Authors:	Duan, Jialong; Institute of Materials Science and Engineering, Ocean University of China, Tang, Qunwei; Institute of Materials Science and Engineering, Ocean University of China, Ocean University of China, He, Belin; Institute of Materials Science and Engineering, Chen, Haiyan; Institute of Materials Science and Engineering,

All-solid-state quantum dot-sensitized solar cell from plastic crystal electrolyte

Jialong Duan, Qunwei Tang*, Benlin He*, Haiyan Chen*

Institute of Materials Science and Engineering, Ocean University of China, Qingdao 266100, P.R.

China;

*Corresponding author: E-mail address: tangqunwei@ouc.edu.cn; blhe@ouc.edu.cn;

chen_hiyan@163.com; Tel/Fax: +86 532 66782533;

Abstract: A plastic crystal based solid-state electrolyte composing of plastic crystal succinonitrile and sodium sulfide (Na_2S) is creatively synthesized by a simple blending approach. The ionic conductivity, charge-transfer ability, and photovoltaic performance are optimized by adjusting succinonitrile/ Na_2S ratio. An optimal power conversion efficiency of 1.29% is measured for its quantum dot-sensitized solar cell (QDSSC) under one sun irradiation. The impressive efficiency along with simple preparation of the cost-effective Na_2S integrated succinonitrile electrolytes highlights the potential application of plastic crystal electrolytes in solid-state QDSSCs.

1 Introduction

Quantum dot-sensitized solar cell (QDSSC) is a competitive photovoltaic conversion device in comparison to dye-sensitized solar cells (DSSCs) because of its superiorities in high theoretical efficiency, cost-effective constituents, and scalable photosensitizers.¹⁻⁵ A typical QDSSC device is comprised of FTO glass supported TiO_2 anode, CdS quantum dot, liquid electrolyte containing $\text{S}^{2-}/\text{S}_n^{2-}$ redox couples, and metal sulfide counter electrode. Similar to liquid-state DSSC,

state-of-the-art QDSSC also meet a persistent problem in encapsulating liquid electrolyte, considerably hindering the long-term stability of the photovoltaic performances. In order to addressing this problem, significant achievements have been made by employing the quasi-solid-state and solid-state electrolytes. For example, the gel electrolytes from the mesoporous silica nanoparticles⁶ and polyacrylamide⁷ have displayed the high charge transfer ability similar to that of liquid electrolyte. Although the photovoltaic performances of the quasi-solid-state QDSSCs have been markedly enhanced, the long-term stability is still unsatisfactory. Solid-state electrolytes are widely considered as promising candidates for markedly enhancing the durability of QDSSCs.⁸ In recent researches, solid-state organic hole-transporting materials such as [2,2',7,7'-tetrakis (N,N-di-p-methoxyphenylamine) -9,9'-spirobifluorine] (spiro-MeOTAD)⁸, poly(3-hexylthiophene) (P3HT)⁹, poly(3,4-ethylene -dioxythiophene) (PEDOT)¹⁰, and inorganic p-type materials such as CuSCN¹¹ have been explored to substitute the liquid electrolyte. However, so far, the solid-state QDSSCs have still shown much lower efficiency because of the mass transport limitation of current electrolytes.^{12,13}

By addressing this issue, we forward here an avenue of designing plastic crystal based all-solid-state electrolyte employing succinonitrile matrix. Plastic crystals are compounds having rotational disorder for molecules or ions and occupied ordered sites by mass centers in their crystalline lattice structures.¹⁴ High ionic conductivity is highlighted in these rotator phases with solid-solid transitions below the melting point. Succinonitrile,¹⁵ a typical molecular plastic crystal, suffers from a first-order transition to a plastic phase at -40 °C and subsequent a body-centered cubic structure at 58 °C. The two identical gauche and one trans isomer conformers in succinonitrile are featured by acceleration in molecular or ion diffusivity. This promising peculiarity triggers our interest in the concept of fast S^{2-}/S_n^{2-} diffusion in succinonitrile. Here we communicate our

preliminary results which support this concept. The solid–state electrolyte described displays high ionic conductivity to be of relevance to solid QDSSC application. To our best knowledge, metal sulfide or selenide compounds are promising materials for quantum dot–sensitized solar cell. However, due to the probability of the electron returning back from polysulfide redox level to metal sulfide valance band, leading to increasing recombination rate in the polysulfide electrolyte/counter electrode interface of QDSSC and decreasing rate of electrocatalyst activity.¹⁶ Aiming to improve the performance of the devices based on the solid–state electrolyte, transparent CoSe alloy counter electrode with fascinating electronic conduction and electrocatalytic ability is utilized to replace the traditional metal sulfides.¹⁷

2 Experimental

2.1 Synthesis of solid–state electrolytes

The plastic crystal electrolyte was made by mixing succinonitrile and Na₂S in a molar ratio of 1:1, 2:1, 4:1, 6:1, or 8:1, and the mixture was heated to ~65 °C with vigorous agitating for 5 h to form the viscous reactant. The resultant solid electrolytes were nominated as succinonitrile/Na₂S, 2succinonitrile/Na₂S, 4succinonitrile/Na₂S, 6succinonitrile/Na₂S, and 8succinonitrile/Na₂S, respectively.

2.2 Synthesis of CoSe alloy counter electrode

The feasibility of synthesizing CoSe alloy CEs was confirmed by following experimental procedures: A mixing aqueous solution consisting of Se powders and CoCl₂ was made by agitating 0.01 g of Se ultrafine powers and 0.0238 g of CoCl₂·6H₂O in 27.5 ml deionized water. 7.5 ml of hydrazine hydrate (85 wt%) was dropped into the above solution, after vigorous agitating for 10 min, the reactant was transferred into a 50 ml of Teflon–lined autoclave and cleaned FTO glass

substrate (sheet resistance $12 \Omega \text{ square}^{-1}$, purchased from Hartford Glass Co., USA) with FTO layer downward was immersed in. After the reaction at $120 \text{ }^\circ\text{C}$ for 12 h, the FTO substrate was rinsed by deionized water and vacuum dried at $50 \text{ }^\circ\text{C}$.

2.3 Assembly of QDSSCs

A layer of TiO_2 nanocrystal anode film with a thickness of $\sim 10 \mu\text{m}$ was prepared by a sol-hydrothermal method.¹⁸ Resultant anodes were alternatively soaked in $0.1 \text{ M Cd}(\text{NO}_3)_2$ ethanol solution for 1.5 min and $0.1 \text{ M Na}_2\text{S}$ methanol solution for 1.5 min. By repeating these cycles for 12 times to obtain CdS sensitized TiO_2 anodes. Then, the solid electrolyte was casted onto CdS-sensitized TiO_2 anode for consolidation at room temperature. The QDSSC was fabricated by sandwiching plastic crystal electrolyte between a CdS-sensitized TiO_2 anode and a CoSe counter electrode, as shown in Fig. 1.

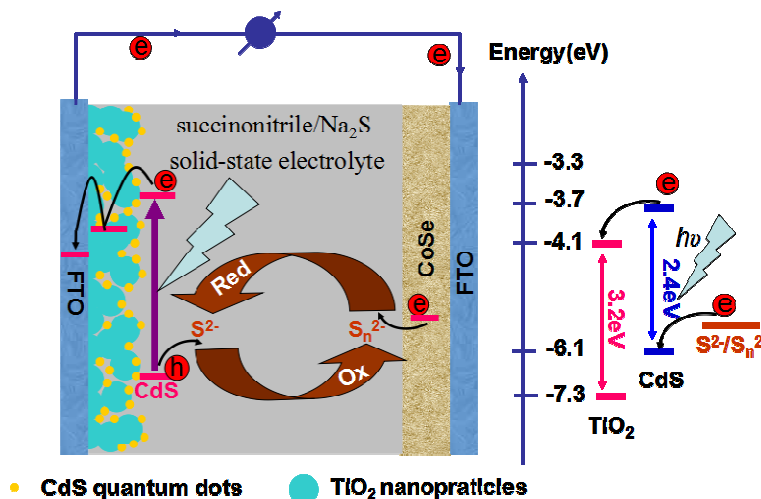


Fig. 1 Schematic diagram for the solid-state QDSSC device.

2.4 Photovoltaic measurements

The photovoltaic test of the QDSSC with an active area of 0.25 cm^2 was carried out using a CHI660E Electrochemical Workstation under irradiation of a simulated AM1.5 solar light from a 100 W Xenon arc lamp (XQ-500 W) in ambient atmosphere.

2.5 Other characterizations

The ionic conductivity of solid electrolyte was measured by using a pocket conductivity meter (DSSJ-308A, LeiCi Instruments). The instrument was calibrated with 0.01 M KCl aqueous solution prior to experiments.

3 Results and discussion

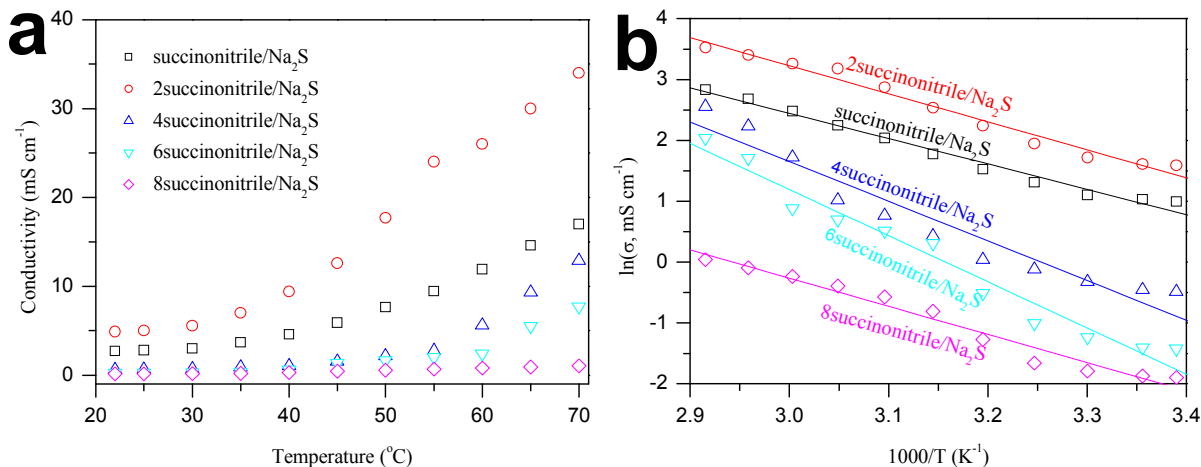


Fig. 2 (a) Conductivity—temperature (σ - t) and (b) $\ln\sigma$ - $1/T$ plots for the solid electrolytes at various stoichiometries.

Fig. 2a shows the temperature dependence of ionic conductivities for the plastic crystal electrolytes. Solid electrolyte from 2succinonitrile/Na₂S display the highest conductivity, which is 5.1 mS cm⁻¹ at 25 °C and it is ~34.0 mS cm⁻¹ at 70 °C. The high conductivity is attributed to the high diffusion capacity of three conformers in succinonitrile, in which trans isomers act as “impurities” and create monovacancies in the lattice, leading to the high molecular diffusivity.¹⁹ Meanwhile, the highest ionic conductivity from 2succinonitrile/Na₂S may generate from the formation of crystal structure due to the interaction between Na atom and N atom of the nitrile group²⁰ and the more free S²⁻ ionic can transfer rapidly along the crystal structure. According to previous studies, the melting point of succinonitrile will be decreased with dopant, such as the succinonitrile doping with N-methyl-N-butylpyrrolidinium iodide.²¹ From the Figure 2a, the temperatures of the ionic

conductivities beginning to increase rapidly decrease from ~ 58 °C to ~ 40 °C with doping more Na_2S into succinonitrile.

By plotting $\ln\sigma$ against $1000/T$, as shown in Fig. 2b, we find the ionic conductivities of the electrolytes follow an Arrhenius relationship: $\sigma = \sigma_0 \exp(-E_a/RT)$, where σ is ionic conductivity, E_a represents activation energy. The straight line for $\ln\sigma-1/T$ plot suggests a typical ion-conducting behavior. The E_a ,²² which is the minimum energies required for ionic conduction through plastic crystal based solid-state electrolytes are obtained from the slopes in the linear fit, showing 38.29, 34.66, 54.23, 63.03, and 38.48 kJ mol^{-1} , respectively. The lowest E_a for 2succinonitrile/ Na_2S electrolyte indicates that charge (S^{2-} and S_n^{2-}) movement becomes easier in plastic crystal system.

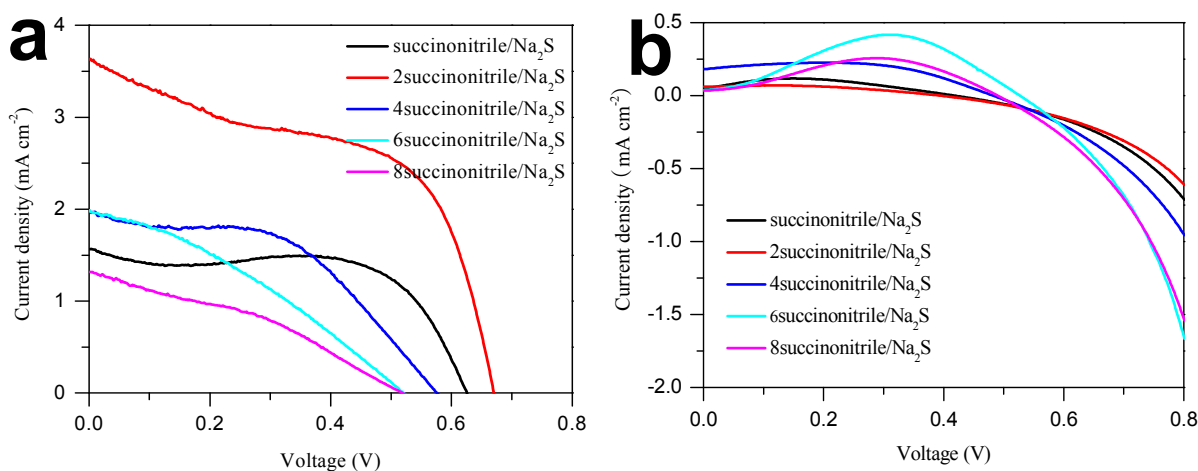


Fig. 3 Characteristic $J-V$ curves of the QDSSCs with solid electrolytes (a) under one sun irradiation and (b) in the dark.

Table 1 Photovoltaic and electrochemical parameters for the QDSSCs with plastic crystal electrolytes.

Plastic electrolytes	crystal	η (%)	J_{sc} (mA cm^{-2})	V_{oc} (V)	FF (%)	R_{ct1} ($\Omega \text{ cm}^2$)	R_{ct2} ($\Omega \text{ cm}^2$)	W (F cm^2)
succinonitrile/ Na_2S		0.64	1.58	0.625	64.8	23.2	602.3	46.8
2succinonitrile/ Na_2S		1.29	3.65	0.670	52.7	3.9	328.3	21.6
4succinonitrile/ Na_2S		0.56	1.95	0.576	49.8	28.1	1019	33.1
6succinonitrile/ Na_2S		0.34	1.97	0.520	33.2	38.5	1599	50.1
8succinonitrile/ Na_2S		0.24	1.31	0.519	35.3	221.6	2290	37.1

Fig. 3a shows the characteristic $J-V$ curves of the QDSSCs with various plastic crystal based solid electrolytes and the photovoltaic parameters are summarized in Table 1. From the data, we can find a regular that the η increases by elevating succinonitrile/ Na_2S molar ratio from 1:1 to 2:1 and subsequently decreases beyond 2:1. The QDSSC with 2succinonitrile/ Na_2S electrolyte yields an optimal η of 1.29% ($J_{\text{sc}} = 3.65 \text{ mA cm}^{-2}$, $V_{\text{oc}} = 0.670 \text{ V}$, $FF = 52.7\%$), which is much higher than the previously reported values.^{23,24} It is noteworthy to mention that J_{sc} has a peak value for the cell with 2succinonitrile/ Na_2S . This may be attributed to a fact that the rapid interconversion between S_n^{2-} and S^{2-} can accelerate the generation of photoelectrons from CdS quantum dots and therefore elevate the electron flow from CdS to conduction band of TiO_2 and accumulative electron density on conduction band of TiO_2 . From the dark $J-V$ curves in Fig. 3b, one can see that the QDSSC with 2succinonitrile/ Na_2S electrolyte has the smallest dark current density at the same voltage. The dark current in a QDSSC is attributed to the combination of S_n^{2-} species with electrons in the CB of TiO_2 at the $\text{TiO}_2/\text{electrolyte}$ interface. The smaller dark current means that the reduction of S_n^{2-} at $\text{TiO}_2/\text{electrolyte}$ interface is retarded. This is another factor for an elevated J_{sc} value for the cell with 2succinonitrile/ Na_2S plastic crystal. It is noteworthy that there is still a dark current when the light is switched off. This result indicates that a galvanic cell may exist in our system. The parallel phenomenon is discovered in dye-sensitized solar cells based on metal wire/ ZnO nanowire arrays.²⁵

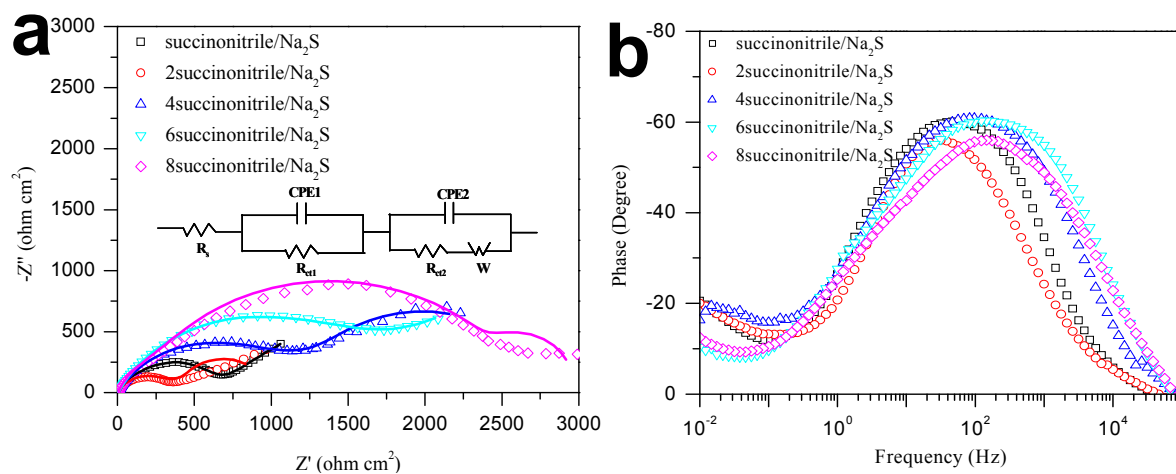


Fig. 4 (a) Nyquist and (b) Bode EIS spectra for the QDSSCs with various solid electrolytes.

Electrochemical impedance spectroscopy (EIS) was performed to evaluate the electrochemical performances of the QDSSCs. Fig. 4a shows the Nyquist plots for the cell devices, giving two semicircles which are assigned to the electrochemical reaction at electrolyte/CoSe counter electrode interface (a smaller one in high frequency region) and charge transfer at CdS–TiO₂/electrolyte (a larger one in low frequency region). An equivalent circuit (see the inset of Fig. 4a) is employed to fit the Nyquist plots for estimating the electrochemical parameters, such as series resistance (R_s), charge–transfer resistance at electrolyte/CoSe counter electrode interface (R_{ct1}), charge–transfer resistance at CdS–TiO₂/electrolyte interface (R_{ct2}), and Nernst diffusion impedance corresponding to diffusion resistance of S_n^{2-}/S^{2-} redox couples (W). CPE1 and CPE2 are constant phase elements. Both R_{ct1} and R_{ct2} have peak valley for 2succinonitrile/Na₂S electrolyte as shown in Table 1, indicating that the plastic crystal electrolyte has the highest charge–transfer ability. The reduction of R_{ct1} and R_{ct2} for 2succinonitrile/Na₂S electrolyte can be attributed to the enlargement of the ionic conductivity. The charge–transfer kinetics of the electrolytes is cross–checked by electron lifetime (τ) at CdS–TiO₂/electrolyte interface.²⁶ In a real QDSSC, the electrons excited from CdS quantum dots will be injected to the conduction band of TiO₂ nanocrystallite, therefore, the τ is positively corrected to charge–transfer ability. Due to the values of R_{ct1} are far less than the R_{ct2} within QDSSCs employing the solid electrolytes, the peaks in high frequency region are hardly discovered. From Fig. 4b, the τ values are calculated by equation:²⁷ $\tau = 1/2\pi f$, where f is the peak frequency attributing to electrochemical reaction at CdS–TiO₂/electrolyte interface. The obtained τ follows an order of 2succinonitrile/Na₂S (6.1 ms) > succinonitrile/Na₂S (3.4 ms) > 4succinonitrile/Na₂S (1.9 ms) > 6succinonitrile/Na₂S (1.3 ms) > 8succinonitrile/Na₂S (1.1 ms), which is consistent with photovoltaic performances of QDSSCs. Till now, we can make a conclusion that the

2succinonitrile/ Na_2S electrolyte show optimal ionic conductivity, E_a for charge transfer, lower charge-transfer resistance and diffusion resistance, therefore the QDSSC with 2succinonitrile/ Na_2S electrolyte is expected to have the best efficiency.

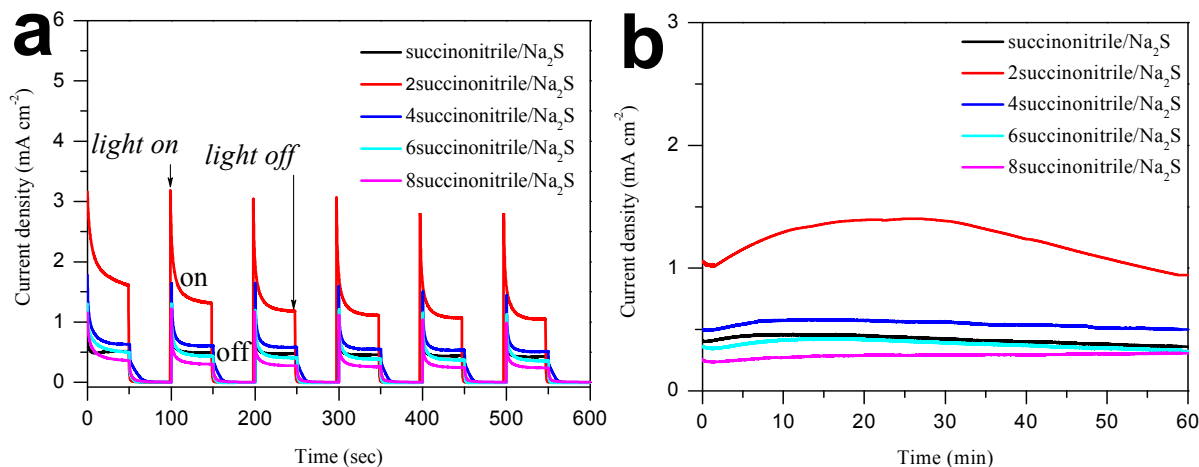


Fig. 5 (a) Start-stop switches of the QDSSCs by alternatively irradiating and darkening the devices, (b) photocurrent stability of the QDSSCs under persistent irradiation.

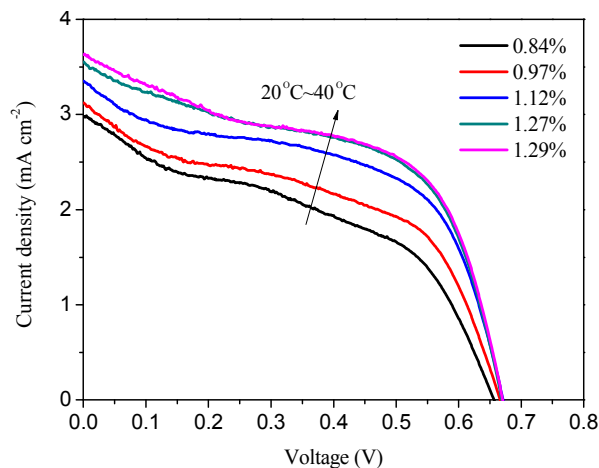


Fig. 6 Characteristic $J-V$ curves of the QDSSC with 2succinonitrile/ Na_2S electrolyte under different temperatures.

The photocurrent dynamics of the solid-state QDSSC was probed in order to determine its start-up, charge diffusion, and photocurrent stability. A fast start-up and long-term stability in engine, vehicle and power source applications have been two challenges for nanoenergy devices.²⁸

Fig. 5a shows the start-up effect in a time slot of 0 ~ 600 s. A sharp increase in photocurrent density

suggests a quick start of cell operation under irradiation, indicating the rapid excitation of CdS quantum dots and high kinetics in electron transportation. For the quick start-up, fast kinetics at CdS-sensitized TiO₂ anode and CoSe alloy counter electrode are crucial to promote the cell launch. Moreover, a decrease in photocurrent density in each “on” state means a diffusion mechanism for charge transfer, which is in EIS analysis. The photocurrent density versus time plots over 60 min display the photocurrent stability on prolonged exposure to light irradiation (100 mW cm⁻²). As shown in Fig. 5b, the photocurrent densities over 60 min-irradiation nearly remain unchanged in comparison with initial value, referring to a relatively good stability. Notably, the increase process in photocurrent means the temperature increment and therefore charge-transfer acceleration under persistent irradiation. From the *J-V* curves in Fig. 6, the photocurrent density increases with increasing the temperature, leading to the enhanced conversion efficiency. This is in a good agreement with the phenomenon in Fig. 5b.

4 Conclusions

In summary, plastic crystal based solid-state electrolytes from Na₂S integrated succinonitrile featured by high conductivity and charge-transfer ability are fabricated and employed in assembling efficient solid QDSSCs. Due to the superiorities of succinonitrile plastic crystal in accelerating S_n²⁻/S²⁻ migration, the kinetics for S_n²⁻ ↔ S²⁻ interconversion has been markedly enhanced. The QDSSC employing 2succinonitrile/Na₂S plastic crystal electrolyte exhibits an optimal efficiency of 1.29%. The research presented here is far from being optimized but these profound advantages along with cost-effectiveness, mild synthesis, and scalable materials promise the succinonitrile/Na₂S plastic crystal electrolytes to be strong candidates in full-solid-state QDSSCs.

Acknowledgements

The authors would like to acknowledge financial supports from Fundamental Research Funds for the Central Universities (201313001, 201312005), Shandong Province Outstanding Youth Scientist Foundation Plan (BS2013CL015), Shandong Provincial Natural Science Foundation (ZR2011BQ017), and Research Project for the Application Foundation in Qingdao (13-4-198-jch).

References

- 1 H. Kim, I. Hwang and K. Yong, *ACS Appl. Mater. Interfaces*, 2014, **6**, 11245.
- 2 W. Ke, G. Fang, H. Lei, P. Qin, H. Tao, W. Zeng, J. Wang and X. Z. Zhao, *J. Power Sources*, 2014, **248**, 809.
- 3 X. Yu, J. Zhu, Y. Zhang, J. Weng, L. Hu and S. Y. Dai, *Chem. Commun.*, 2012, 48, 3324.
- 4 C. F. Du, T. You, L. Jiang, S. Q. Yang, K. Zou, K. L. Han and W. Q. Deng, *RSC Adv.*, 2014, **4**, 33855.
- 5 K. Yu, X. Lin, G. Lu, Z. Wen, C. Yuan and J. Chen, *RSC Adv.*, 2012, **2**, 7843.
- 6 H. W. Chen, Y. D. Chiang, C. W. Kung, N. Sakai, M. Ikegami, Y. Yamauchi, K. C. Wu, T. Miyasaka and K. C. Ho, *J. Power Sources*, 2014, 245, 411.
- 7 Z. X. Yu, Q. X. Zhang, D. Qin, Y. H. Luo, D. M. Li, Q. Shen, T. Toyoda and Q. B. Meng, *Electrochem. Commun.*, 2010, 12, 177.
- 8 T. P. Brennan, P. Ardalan, H. B. R. Lee, J. R. Bakke, I-K. Ding, M. D. McGehee and S. F. Bent, *Adv. Energy Mater.*, 2011, **1**, 1169.
- 9 J. A. Chang, J. H. Rhee, S. H. Im, Y. H. Lee, H. Kim, S. I. Seok, M. K. Nazeeruddin and M. Gratzel, *Nano Lett.*, 2010, 10, 2609.

- 10 J. Xia, N. Masaki, M. Lira-Cantu, Y. Kim, K. Jiang and S. Yanagida, *J. Am. Chem. Soc.*, 2008, **130**, 1258.
- 11 B. C. Lévy-Clément, R. Tena-Zaera, M. A. Ryan, A. Katty and G. Hodes, *Adv. Mater.*, 2005, **17**, 1512.
- 12 J. Qian, Q. S. Liu, G. Li, K. J. Jiang, L. M. Yang and Y. Song, *Chem. Commun.*, 2011, **47**, 6461.
- 13 P. K. Singh, K. W. Kim and H. W. Rhee, *Electrochem. Commun.*, 2009, **11**, 1247.
- 14 C. A. Angell, *J. Non-Cryst. Solids*, 1991, **131–133**, 13–31.
- 15 T. Bischofberger and E. Courtens, *Phys. Rev. Lett.*, 1974, **32**, 163.
- 16 M. Eskandari, V. Ahmadi and R. Ghahary, *Electrochimica Acta*, 2015, **151**, 393.
- 17 J. L. Duan, Q. W. Tang, R. Li, B. L. He, L. M. Yu and P. Z. Yang, *J. Power Sources*, 2015, **284**, 369.
- 18 B. B. Hu, Q. W. Tang, B. L. He, L. Lin and H. Y. Chen, *J. Power Sources*, 2014, **267**, 445.
- 19 Q. Dai, D. R. MacFarlane, P. C. Howlett and M. Forsyth, *Angew. Chem.*, 2005, **117**, 317.
- 20 H. X. Wang, H. Li, B. F. Xue, Z. X. Wang, Q. B. Meng and L. Q. Chen, *J. Am. Chem. Soc.*, 2005, **127**, 6394.
- 21 P. Wang, Q. Dai, S. M. Zakeeruddin, M. Forsyth, D. R. MacFarlane and M. Grätzel, *J. Am. Chem. Soc.*, 2004, **126**, 13590.
- 22 Q. W. Tang, S. S. Yuan and H. Y. Cai, *J. Mater. Chem. A*, 2013, **1**, 630.
- 23 I. Barcelo, J. M. Campina, T. Lana-Villarreal and R. Gomez, *Phys. Chem. Chem. Phys.*, 2012, **14**, 5801.
- 24 C. F. Chi, P. Chen, Y. L. Lee, I. P. Liu, S. C. Chou, X. L. Zhang and U. Bach, *J. Mater. Chem.*, 2011, **21**, 17534.

25. W. Wang, Q. Zhao, H. Li, H. W. Wu, D. C. Zou and D. P. Yu, *Adv. Funct. Mater.*, 2012, **22**, 2775.
26. J. Liu, Q. W. Tang and B. L. He, *J. Power Sources*, 2014, **268**, 56.
27. R. Gao, L. Wang, B. Ma, C. Zhan and Y. Qiu, *Langmuir*, 2010, **26**, 2460.
28. C. Laberty–Robert, K. Vallé, F. Pereira and C. Sanchez, *Chem. Soc. Rev.*, 2011, **40**, 961.

